A Numerical Study of Debye and Conductive Dispersion in High Dielectric Materials Using a General ADE-FDTD Algorithm

D. R. Gibbins, C.J. Railton, *Member, IEEE*, I. J. Craddock, *FIEEE*, T. N. T. Henriksson

***Abstract*— A new formulation of the Auxiliary Difference Equation (ADE) Finite Difference Time Domain (FDTD) algorithm for the simulation of dispersive materials has been presented in the literature. Although flexible and efficient, this algorithm suffers from instability when modelling lossy high contrast dielectrics.**

In this paper we adapt this ADE-FDTD formulation and present alternative algorithms for modelling static conductivity and Debye dispersion. The stability of these algorithms is assessed by numerical simulation in a wide variety of dielectric media and their performance is compared to the existing algorithm by means of a simulation of the reflection of a plane wave from a dielectric boundary. Results and comparison with theory demonstrate the stability and accuracy of the new methods. The flexibility, computational efficiency and ability to model a wide range of materials make these new methods highly attractive compared to other dispersive FDTD algorithms, particularly for modelling materials with multiple dispersion models.

***Index Terms*—FDTD methods, electromagnetic propagation in dispersive media, dispersive media.**

I. Introduction

IN most instances the Finite Difference Time Domain (FDTD) method is used to model materials with frequency-independent values of permittivity. In cases when a large frequency bandwidth or highly lossy materials are to be investigated, it often becomes necessary to model their frequency-dependent or dispersive behavior; this may require the combination of a number of different dispersion models. A classic example of this is the use of the Stogryn model [1] that combines Debye and static conductive dispersion to model the properties of saline water. This same model can be used as an approximation of biological tissues at microwave frequencies [2]

There are a number of different methods available that allow the simple "Yee" form of the FDTD equations [3] to be modified, enabling dispersive behavior to be modelled. These can be grouped into three main types; Z-transform methods that make use of digital filtering theory [4]; methods based on the discrete convolution of the dispersion relation in the time domain [5]; and those that employ the Auxiliary Differential Equation (ADE) approach [6]-[11]. The ADE method offers a more general, flexible implementation of the dispersion relation that lends itself to modelling arbitrary permittivity functions

[6].

In general ADE algorithms need a different formulation for each type of dispersion and for multi-pole materials the calculation can become complicated and cumbersome. In [5]

TABLE I
ALGORITHMS DISCUSSED IN THIS ARTICLE

ALGORITHM NAME	ALGORITHM DESCRIPTION
E-FIELD UPDATE ALGORITHMS	
E-field update 1	Original two part ADE E-field update as presented in [5]
E-field update 2	New two part E-field update that uses ETD to incorporate static conductivity into part 1 of the update in the calculation of *D*
P-FIELD UPDATE ALGORITHMS	
ATD update	Equation for polarization density, presented in [5], that uses approximate time differencing to unify all forms of dispersion into a single, general formulation
ETD Debye update	Update equation for Debye type dispersion polarization density formulated using exponential time differencing
RSL conductivity update	Update equation for effective conductivity polarization density formulated using the restart stabilized leapfrog method

Paper submitted first for review on 27th March 2014,

D R Gibbins is currently with Toshiba Research Laboratory, 32 Queen Square, Bristol, UK, BS1 4ND (david.gibbins@toshiba-trel.com).
C.J. Railton was formally with the Department of Electrical and Electronic Engineering, University of Bristol Marchant Venturers Building, Woodland Road, BS8 1UB, Bristol, UK.
I. J. Craddock is currently with Toshiba Research Laboratory, 32 Queen Square, Bristol, UK, BS1 4ND and the Department of Electrical and Electronic Engineering, University of Bristol Marchant Venturers Building, Woodland Road, BS8 1UB, Bristol, UK. (Ian.Craddock@toshiba-trel.com).
T. N. T. Henriksson is currently with the Department of Electrical and Electronic Engineering, University of Bristol Marchant Venturers Building, Woodland Road, BS8 1UB, Bristol, UK (fetnth@bristol.ac.uk).

an ADE FDTD formulation is presented that allows complex media to be modelled using the same general form. Multiple dispersion types or poles can be included by adding additional polarization density (*P*) terms to the update equations. The algorithm is based on the idea of splitting the E-field FDTD update into two parts. In part 1 the Electric displacement (*D*) is calculated from the magnetic (*H*) fields using the standard Yee equation. In part 2 the E-field is calculated from *D* and *P*, using a permittivity model that includes the effects of dispersion. In addition a general formulation for the FDTD update equations for *P* is presented that unifies all the different dispersion models e.g. Lorentz, Drude and Debye, into a single form. The formulation is flexible and computationally efficient. However, when modeling high loss and/or large dielectric contrasts it becomes unstable.

In this paper we introduce new time update equations for *P* for static conductivity (P_σ) and Debye dispersion (P_d) that are stable in such conditions. The numerical update for P_d is derived using the using the Exponential Time Differencing (ETD) [12] method to solve the differential time domain Debye susceptibility equation. The update for P_σ is derived using the Restart Stabilized Leapfrog (RSL) [13] method in a similar fashion. In addition a new ADE formulation is presented that is also capable of simulating high loss materials in which the standard lossy ETD FDTD equations are extended to incorporate the effects of dispersion. While not as processor-efficient the new ETD-ADE formulation is more memory-efficient than the RSL implementation of static conductivity. A summary of the algorithms discussed in this paper can be seen in Table I.

II. ADE-FDTD EQUATIONS

The complete two part E-field update presented in [6] at iteration *n* of the ADE-FDTD algorithm is given by:

$$D^{n+1} = D^n + \Delta(\nabla \times H)^{n+1/2} \tag{1}$$

$$E^{n+1} = \frac{\mathrm{D}^{n+1} - \sum_{i=1}^{I} P_i^{n+1}}{\varepsilon_0 \varepsilon_\infty} \tag{2}$$

Where $\nabla \times H$ is the curl of the H-fields, Δ is the FDTD time-step, P_i^n is the polarisation density contribution from polarization term *i*, ε_0 is the permittivity of free space and ε_∞ is the relative permittivity when the angular frequency $\omega = \infty$. Henceforth the update equation for *D* in (1), will be referred to as *part* 1 of the update scheme, the update equation in (2) will be referred to as *part 2* while the combination of (1) and (2) will be referred to as *E-field update 1*.

A previous attempt [6] has been made to produce a general formulation for the time domain update equations for *P* that unifies the all the different dispersion models e.g. Lorentz, Drude and Debye, into a single form. The resulting update equation is given by:

$$P^{n+1} = C_1 P^n + C_2 P^{n-1} + C_3 E^n \tag{3}$$

where the coefficients C_1, C_2 and C_3 are calculated as:

$$C_1 = \frac{4d - 2b\Delta^2}{2d + c\Delta} \tag{4}$$

$$C_2 = \frac{-2d - c\Delta}{2d + c\Delta} \tag{5}$$

$$C_3 = \frac{2a\Delta^2}{2d + c\Delta} \tag{6}$$

The constants *a, b, c* and *d* are determined by the dispersion type and are found by comparing the frequency domain form of the polarization density for the particular dispersion model with the general form:

$$P(\omega) = \frac{a}{b + j\omega c - d\omega^2} E(\omega) \tag{7}$$

For more details of this derivation see [6]. Due to the way that the time derivatives are approximated to obtain equations (4) to (6), this formulation of the update equations for *P* (henceforth referred to as the Approximate Time Derivative (ATD) method) results in solutions that become unstable for high values of permittivity as shown in the results section.

A. Stable time domain ADE algorithm for static conductivity using ETD

In this section an alternative 2-part derivation for the E-field update equations is presented. In this new form the contribution from static conductivity is incorporated into *part 1* of the update, rather than being treated as a polarization density term and included in *part 2* of the update as is done in *E-field update 1*. The starting point for deriving *part 1* of the update equation is:

$$\nabla \times H(t) = \sigma E(t) + \frac{\partial D(t)}{\partial t} \tag{8}$$

In order to find a numerical solution to this equation it must be in the form of a first order Ordinary Differential Equation (ODE) in terms of *D(t)*. In this form the equation may be solved using one of a number of different techniques including linearly implicit methods [14], projection methods [15] or Exponential Time Differencing (ETD) methods [12]. Of these ETD has already been used to produce an alternative formulation of the basic lossy FDTD algorithm [17] and generally produces high accuracy, stable solutions. To obtain the correct form the right hand side of the equation needs to be expressed in terms of *D*(*t*) and so an equation is required relating $\sigma E(t)$ to *D*(*t*). Multiplying both sides of the non-discretized version of (2) by the conductivity provides this relationship:

$$\sigma E(t) = \frac{\sigma}{\varepsilon_0 \varepsilon_\infty} \left(\mathrm{D(t)} - P_{sum}(t) \right) \tag{9}$$

Where the term $P_{sum}(t) = \sum_{i=1}^{I} P_i(t)$, the total polarization density, is introduced for clarity. Substituting this result into (8) and grouping *D(t)* terms on the right hand side gives:

$$\frac{\partial D(t)}{\partial t} + \frac{\sigma}{\varepsilon_0 \varepsilon_\infty} D(t) = \nabla \times \mathrm{H(t)} + \frac{\sigma}{\varepsilon_0 \varepsilon_\infty} P_{sum}(t) \quad (10)$$

This equation is now in the form of an ODE that can be solved for *D* using the ETD method. The detail of this process can be seen in appendix A. The resulting numerical solution is:

$$D^{n+1} = D^n e^{\frac{-\sigma\Delta}{\varepsilon_0 \varepsilon_\infty}} + \frac{\varepsilon_0 \varepsilon_\infty}{\sigma}\left(1 - e^{\frac{-\sigma\Delta}{\varepsilon_0 \varepsilon_\infty}}\right) \ldots \times \left(\nabla \times \mathrm{H}^{n+\frac{1}{2}} + \frac{\sigma}{\varepsilon_0 \varepsilon_\infty} P_{sum}^{n+\frac{1}{2}}\right) \quad (11)$$

The $P^{n+\frac{1}{2}}$ term in this equation is not directly available as it is calculated at the same time intervals as the E-field, but it can be approximated by averaging the polarization field values at *n* and *n*+1:

$$P^{n+\frac{1}{2}} = \frac{(P_{sum}^{n+1} + P_{sum}^{n})}{2} \quad (12)$$

Applying this averaging gives the final update equation for *D*:

$$D^{n+1} = D^n e^{\frac{-\sigma\Delta}{\varepsilon_0 \varepsilon_\infty}} + \frac{\varepsilon_0 \varepsilon_\infty}{\sigma}\left(1 - e^{\frac{-\sigma\Delta}{\varepsilon_0 \varepsilon_\infty}}\right) \ldots \times \left(\nabla \times \mathrm{H}^{n+\frac{1}{2}} + \frac{\sigma}{2\varepsilon_0 \varepsilon_\infty}(P_{sum}^{n+1} + P_{sum}^{n})\right) \quad (13)$$

This equation forms *part 1* of the E-field update. The D^{n+1} calculated here is used in conjunction with *part 2* of the original formulation (2) to complete the E-field update. It should be noted that if modelling only static conductivity with no other forms of dispersion i.e. $P_{sum} = 0$, the equation reduces to the standard ETD-FDTD equation for D. From this point on the E-field update that comprises (13) (part 1) and (2) (part 2) will be referred to as *E-field update 2*.

B. Stable time-domain update for static conductivity polarization density

E-field update 1 can also be used to simulate the effects of static conductivity by representing it as an effective polarization density term P_σ in *part 2*, equation (2). Although the ATD formulation can be used to produce such an update this becomes unstable in highly lossy conditions (see section IV). A new derivation for P_σ is now presented that is stable in such conditions. The time domain equation for the conductivity term is given by:

$$\frac{\partial P_\sigma(t)}{\partial t} = \sigma E(t) \quad (14)$$

The most basic solution to this equation is found using Euler's method [13]. This is the simplest example of the Runga-Kutta class of numerical methods for solving differential equations. Using the Euler method an update of length Δ is calculated from the solution at (*n*-1) using the gradient at the same point. When applied to (14) Euler's method gives the update for P_σ at the nth time step, as:

$$P_\sigma{}^{n+1} = P_\sigma{}^{n} + \Delta\sigma E^n \quad (15)$$

The Euler method is 1st order accurate and uses derivative information from only the beginning of the interval. As a result, the local step error is $O(\Delta^2)$ while the global error is $O(\Delta)$. This method is considered to be neither very accurate nor very stable when compared to other methods using the same step size.

An alternative numerical technique is the Leapfrog method [13]. Used by Yee to produce the original FDTD equations [3] this method is of the 2nd order Runga-Kutta class and amounts to solving an initial value problem for a system of ODE's with the Mid-Point (MP) method [13]. Specifically, the solution at iteration n is found using an update 2Δ in length from the solution at (*n*-1) based on a derivative calculated at (*n*). This progression can conveniently be started using the Euler method (15). Applying the leapfrog method to (14) gives:

$$P_\sigma{}^{n+1} = P_\sigma{}^{n-1} + 2\Delta\sigma E^n \quad (16)$$

Because the Leapfrog method is 2nd order accurate the local error for this method is $O(\Delta^3)$ and the global error is $O(\Delta^2)$, significantly more accurate than the solution in (15).

Equation (15) is the solution obtained using the ATD formulation (3) and will be referred to as the *ATD conductivity update*. As shown in Section IV, this becomes unstable for large values of σ as the solution tends to drift apart at odd and even time steps, leading to instability and eventually rapid divergence. The Leapfrog method maybe stabilized for practical purposes by "restarting" the sequence every 20 iterations using a single Euler step, realigning the odd and even terms [13]. Using this approach a new update for P_σ, referred to as the Restart Stabilized Leapfrog (RSL), is defined as the Leapfrog solution (16) restarted every 20 iterations with a Euler step (15).

C. Derivation of Stable Debye time update equation for polarization density

The time-domain polarization density for a single Debye pole P(t) is given as [16]:

$$\frac{\partial P(t)}{\partial t} + \frac{1}{\tau} P(t) = \frac{\varepsilon_0(\varepsilon_S - \varepsilon_\infty)}{\tau} E(t) \quad (17)$$

Where ε_s is the static permittivity, and τ is the relaxation time as described above. The term $(\varepsilon_s - \varepsilon_\infty)$ represents the ability of the dipoles responsible for the dispersion to become .

As in the case of (10) this is in the form of an ODE that may be solved using the ETD method to produce a time domain numerical solution for the polarization density (P_d^{n+1}):

$$P_d^{n+1} = P_d^n \cdot e^{\frac{-\Delta}{\tau}} + \varepsilon_0(\varepsilon_s - \varepsilon_\infty)\left(1 - e^{\frac{-\Delta}{\tau}}\right) E^n \quad (18)$$

For detail of this derivation see appendix B. This will be

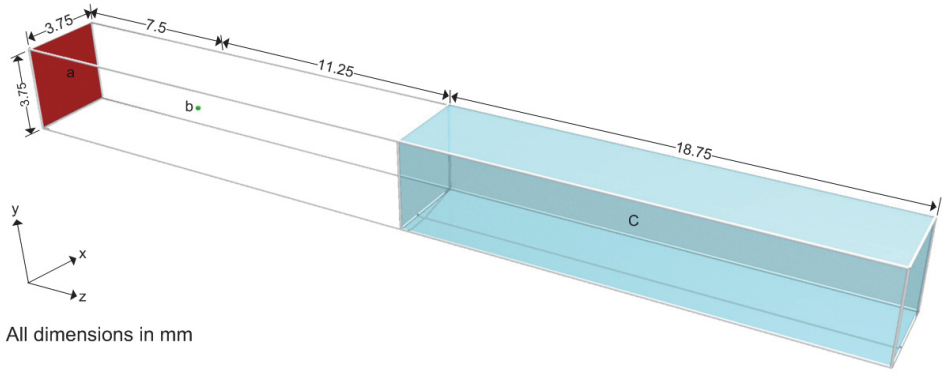

Fig. 1. Numerical FDTD model used to validate the dispersive ADE –FDTD code: a. excitation surface, b. field probe, c. dispersive material

referred to as the *ETD-Debye update*. Comparing this equation with (3) equivalent values of C_1, C_2 and C_3 can be identified and compared with the equivalent coefficients for the ATD-Debye update [6] (see Table II). The fact that C_2 coefficient is zero in the ETD case means that neither a coefficient nor P^{n-1} field values needs to be held in memory resulting in savings in both time and computational costs and a more efficient algorithm compared to the ATD approach. A comparison of the stability of these algorithms can be seen in the results section.

It should be noted that an attempt was made to stabilize the ATD Debye update using an Euler restart. While this proved partially successful in stabilizing the simulation, a shorter time step was required than was prescribed by the Courant stability limited and for large values the simulation still rapidly diverged.

III. Numerical Experiments

To test accuracy and stability of the algorithms presented above a simple numerical experiment was devised. This experiment comprises calculating the reflection coefficient of a plane wave normally incident on a boundary between free space ($\varepsilon = 1, \sigma = 0, \mu = 1$) and a homogeneous, dispersive, non-magnetic ($\mu = 1$) dielectric test material with complex permittivity $\varepsilon_t(\omega)$ and conductivity σ_t.

An FDTD model, shown in Fig. 1, was developed to model this scenario consisting of a workspace (3.75, 3.75, 37.5) mm half of which is free space while the other half (object *c*) is filled with the dispersive test material. The simulation space, delineated by a thick black line, is bounded by a Perfect Electric Conductor (PEC) on the y-direction boundaries, a Perfect Magnetic Conductor (PMC) condition on the x-direction boundaries and Mur's 1st order Absorbing Boundary Condition (ABC) on the z-direction boundaries. A y-direction polarized current source excitation surface is placed at the z-boundary (object *a* in Fig. 1). This surface is excited with a Single Cycle Sinusoid (SCS) time-domain waveform with a width of 50ps and a central frequency of 20GHz. This arrangement ensures that the wave front has the form of a normal plane wave at the material boundary. The model is meshed with 0.0375mm cubic cells and a time interval size (Δ) of 95% of the Courant stability factor for 3D FDTD is used in all simulations [8].

TABLE II
ETD and ATD coefficients for the numerical update of Debye Polarization Density

Coefficient	C_1	C_3	C_2
ETD	$e^{\frac{-\Delta}{\tau}}$	0	$\varepsilon_0(\varepsilon_s - \varepsilon_\infty)\left(1 - e^{\frac{-\Delta}{\tau}}\right)$
ATD	$\frac{-2\Delta}{\tau}$	1	$\frac{2(\varepsilon_s - \varepsilon_\infty)\Delta}{\tau}$

Simulations were run for 1100ps (8000 iterations) during which, the time domain incident fields and fields reflected from the air/test material interface were observed. This simulation time is approximately 5 times longer than that required to observe the return pulse so as to ensure the stability of the simulation of the simulation in the long term. In experiments where Δ was altered the number of iterations was increased to maintain the same run time. The experimental frequency domain reflection coefficient $\rho(\omega)$ was calculated from the Fourier transform of these fields windowed to 300ps (2200 iterations) so as to isolate the response from the material boundary from long term effects such as reflections from the ABC at the end of the *z*+ extreme of the simulation domain.

Three variations of this experiment were carried out (henceforth referred to as Case 1-3) modelling the test material with different material values and algorithms:

Case 1. This tests the implementation of static conductivity using *E-field update 1* and the RSL update for P_σ. A lossy test material was simulated using the RSL algorithm with $\hat{\varepsilon}_t = 1$ and various values of σ. The results of this will be compare to modelling the same material using *E-field update 1* and the *ATD conductivity update*.

Case 2. This tests the implementation of Debye dispersion in conjunction with the *E-field update 1*. In this case the test material properties were based on that of a single-pole Debye model of water ($\varepsilon_\infty = 1.8, \varepsilon_s = 81, \tau = 9.4 \times 10^{-12}$). The value of ε_s was varied in order to access the

stability of the ATD and ETD Debye pole implementations.

Case 3. This tests the implementation of static conductivity using *E-field update 2*. In this case the material simulated is the Debye-dispersion water model in case 2 and also a Debye-dispersion model of methanol ($\varepsilon_\infty = 2.05, \varepsilon_s = 35.5, \tau = 48.3 \times 10^{-12} ps$), both simulated using the ETD - Debye update, but with 1, 5, 10 and 20S/m of additive conductivity. It is necessary to perform the test *for E-field update 2* in conjunction with another dispersion type as without a polarization density term this method reduces to the well-known and well tested ETD-FDTD algorithm [17].

To verify the accuracy of the simulated reflection coefficient, in each case it will be compared with the theoretical reflection coefficient which, for a normal plane wave incident on a boundary between free space and a dielectric medium with a permittivity $\hat{\varepsilon}_d(\omega)$ is given by the

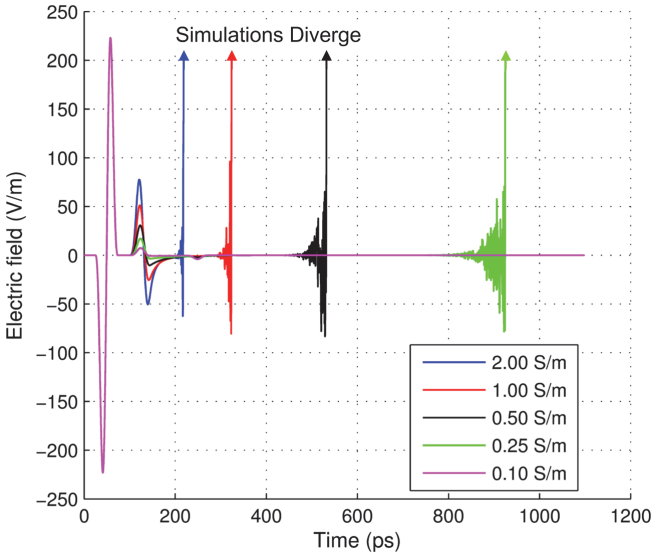

Fig. 2 simulated time domain wave forms illustrating the implementation of conductivity with the RSL and ATD conductivity updates.

equation [18]:

$$\rho(\omega) = \frac{\sqrt{\hat{\varepsilon}_d(\omega)}-1}{\sqrt{\hat{\varepsilon}_d(\omega)}+1} \tag{19}$$

Where $\hat{\varepsilon}_d(\omega)$ is the complex frequency domain permittivity of the test material including a conductive term defined by $\hat{\varepsilon}_d(\omega) = \varepsilon_d(\omega) - \sigma_d/j\omega$.

IV. Results and Discussion

A. Case 1: Static conductivity

Fig. 2 demonstrates the instability seen when performing simulations using the ATD conductivity update. For the range of conductivity values evaluated, both the incident pulse and the inverted pulse reflected from the dielectric boundary are visible. After this point the simulations become unstable and the solution diverges to infinity. The point at which this

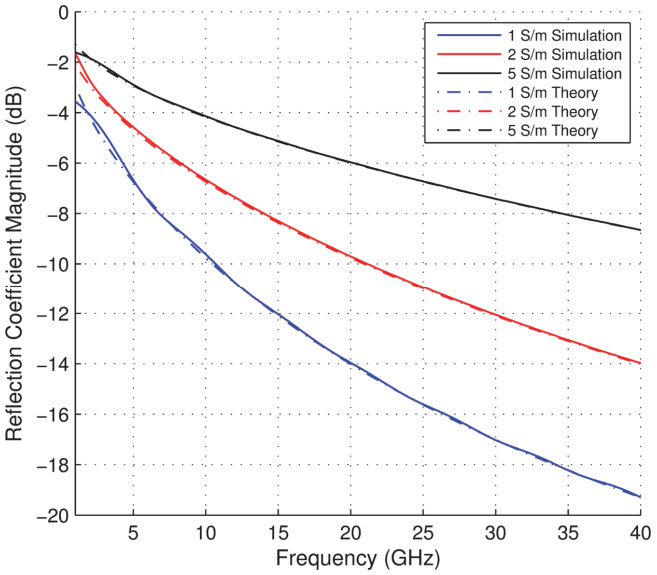

Fig. 3 Comparison of frequency domain reflection coefficient of vacuum – lossy dielectric interface ($\hat{\varepsilon}_t = 1, \sigma_t = 2$) as found via the RSL conductivity algorithm and theory.

happens is dependent on the value of σ, the greater the value the more rapidly the simulation destabilizes. When the ATD simulation was run with $\sigma = 0.1$ the solution remained stable throughout the entire 1100ps of the simulation, though will probably diverge at some point beyond this. Varying the time step used in the simulation between 95% and 15% of the Courant limit, resulted in little change in the point at which the simulations diverged. This indicates that this is not a Courant instability, but a more severe long-term problem likely due to the approximations of the derivatives used to produce the solution (see II.B).

With the introduction of a "restart" into the leapfrog scheme every 20 iterations (RSL update for conductivity - see II.B), the simulations seen in Fig. 2 become stable and all cases run for the full 1100ps without diverging. Fig. 3 demonstrates the ability of this method to model the effects of static conductivity. It shows the frequency domain reflection coefficient of the lossy dielectric interface, obtained from the stable *RSL* waveforms and the equivalent response as calculated by theory. The two responses show a good level of agreement, the simulated response deviating from the predicted value by less than 0.1dB between 5 and 40GHz. At lower frequencies larger differences are probably due to the fact that the wavelength is becoming large in relation to the test setup and boundary effects, not accounted for in the theoretical solution, become more prevalent.

B. Case 2: Simulation of Debye Type Dispersion

Fig 4 shows the time domain fields reflected from various vacuum/material interfaces for case 2. The instability of the ATD formulation for Debye dispersion is demonstrated by simulating five different values of static permittivity, varying from 70 to 5. This corresponds to values of 68.2 – 3.2 for $(\varepsilon_s - \varepsilon_\infty)$, the term driving the Debye pole. The behavior shown is similar to that of the ATD formulation for conductivity; The greater the value of the ε_s term the more

rapidly the simulation diverges.

Varying the time-step between 0.95% and 15% of the Courant stability criterion has a negligible effect on the point at which the simulation becomes unstable. Once again

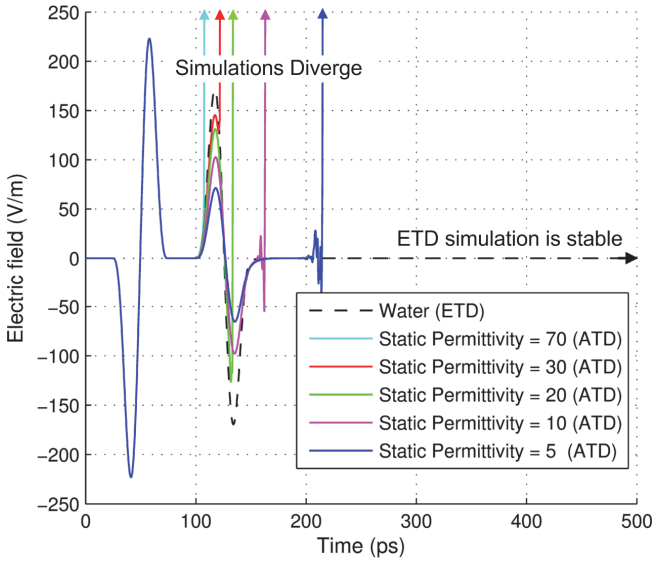

Fig. 4 Simulated time domain wave forms illustrating the reflection from a vacuum/water interface modelled using the ATD and ETD implementation of Debye dispersion.

demonstrating that, rather than being a Courant instability, the volatility of the algorithm is due to an inherent flaw in the formulation of the solution. As the approximations of the derivatives, in this case, are made in the same manner as for the simpler formulation for conductivity, it is reasonable to assume that the instability has the same root cause (see II.B). This confirms that the ATD-Debye algorithm is inappropriate for large dielectric contrasts and more specifically the approximation of the time derivatives in the ATD derivation is not valid.

Fig 4 Also shows the responses for a single-pole Debye water model simulated using the ETD implementation of Debye dispersion. In this case the plot shows the incident pulse as it propagates toward to the interface and the inverted reflected pulse and thereafter tends to zero.

Fig. 5 shows the frequency domain reflection coefficient of the vacuum/water interface as calculated via theory and the Fourier transform of the ETD-Debye waveform in Fig. 4. This shows an excellent level of agreement between the simulated and theoretical values across the entire bandwidth, confirming the ETD–Debye update is a practical implementation of Debye type dispersion.

C. Case 3: Simulation of static conductivity using E-field update 2 with Debye Dispersion

Fig. 5 also shows the reflection coefficient from the combined property interface for water with various levels of additive static conductivity, calculated from simulation and by theory. As expected these responses show more complex behavior than the water seen in case 3 as the conductive component dominates at low frequencies, while at high frequencies the Debye pole dominates and the form is much the same as the case without additive conductivity. In each

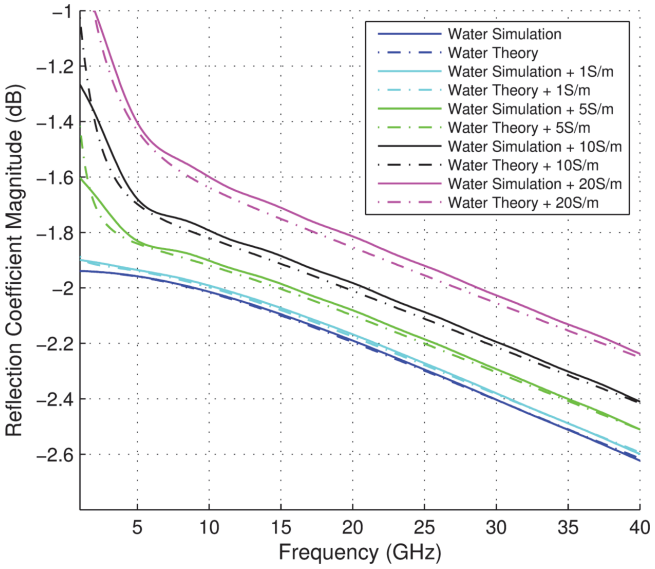

Fig. 5 Comparison of Frequency domain reflection coefficient of vacuum/water interface as found via the ETD stabilized Debye pole with varying amounts of additive static conductivity. Theoretical response denoted by dashed line, FDTD simulation by solid line.

case the response is in good agreement with the theoretical behavior. The main disagreement is that the simulated results exaggerate the effect of conductivity, deviating by a maximum 0.05dB across the 0-40 GHz frequency range for the +20S/m simulation. This difference is likely due to the same modelling errors seen for the *RSL conductivity update* in case 1.

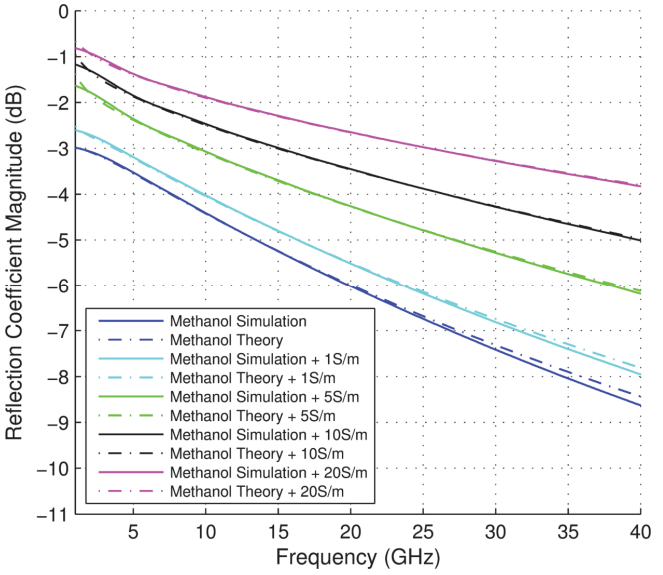

Fig. 6 Comparison of Frequency domain reflection coefficient of vacuum/methanol interface as found via the ETD stabilized Debye pole, with varying amounts of additive static conductivity. Theoretical response denoted by dashed line, FDTD simulation by solid line.

The above experiment was repeated with methanol instead of water. The methanol was modelled using a single Debye

pole. Fig. 6 shows the reflection coefficient calculated by simulation and theory. As for the previous case the results from simulation agree closely with the theoretical values. The methanol only results confirm the efficacy of the *ETD–Debye update* implementation of Debye type dispersion. The additive conductivity results generally show better agreement than those for water, though the maximum deviation occurring at lower frequencies with deviation of 0.2dB for the +10S/m case at 1GHz.

To further test the stability of the combination of the *ETD–Debye update* and *E-field update 2* in different scenarios two further tests were carried out. In the first the planar interface was replace by a 0.5mm radius sphere. This was modelled using the single pole Debye model of water with various

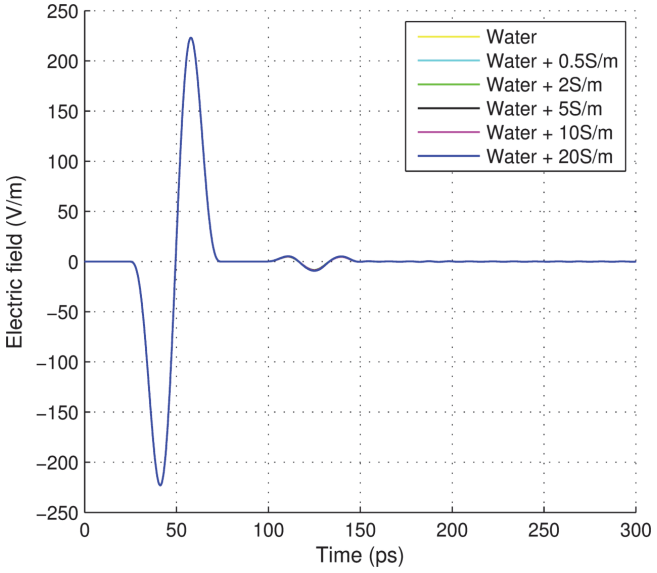

Fig. 7 .Simulated electric field showing an incident pulse (first) and the subsequent return (second) pulse from a sphere of water with varying degrees of additive static conductivity.

levels of additive static conductivity. The resulting time-domain waveforms can be seen in Fig. 7. For all cases the resulting waveforms were very similar and as a result cannot be discerned from one another. Both the incident pulses and smaller return pulses are visible and shaped as expected, while the simulation remained stable after interaction with the sphere tending to zero in the long term.

In a second test of stability the same arrangement was used as in Fig. 1, with the material in object c being modelled with a single pole Debye model of water, with various levels of additive static conductivity. In this case the $z+$ Mur boundary and the $x+$ and $x-$ boundaries, were replace with PEC boundary conditions. Leaving only the $z-$ boundary as a Mur absorbing condition. Removing the absorbing boundary conditions removes their damping effect on the electric field in the simulation, testing the stability of the algorithm in the most extreme conditions. This simulation was run for a total of 16000 iterations or 2200ps twice that of the previous simulations.

The results of this experiment can be seen in Fig. 8. As for the case of the sphere, all plots are very similar. The resonance within the simulation volume, caused by removing the absorbing boundary conditions, can clearly be seen, but the field remains dynamically stable for the whole simulation time, tending towards zero after some initial fluctuation caused by the interaction with the material interface.

These results demonstrate the accuracy of the *ETD–Debye update* and *E-field update 2* combination across a wide range of frequencies and material parameters and the stability of the algorithm in different simulation scenarios.

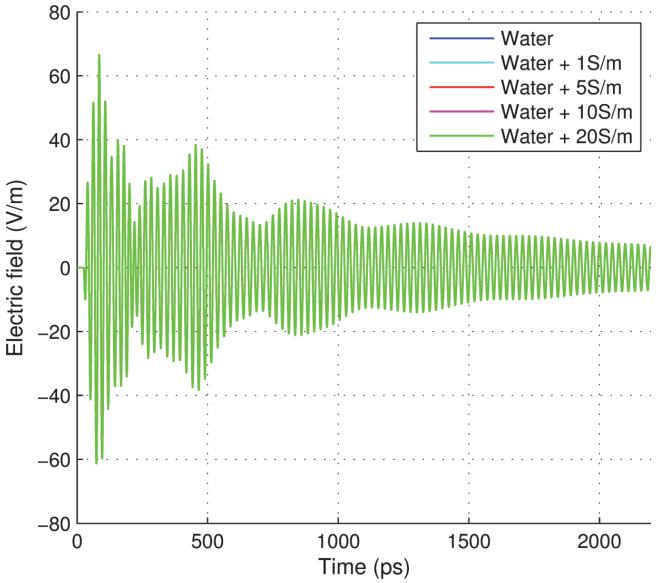

Fig. 8 .Simulated electric field at field probe (b. in Fig. 1) for case when all but the z- boundary are set as PEC.

Both *E-field update 2* and the *RSL conductivity update*/ *E-field update 1* implementations of conductivity have been shown to be practicable implementations of static conductivity. In terms of computational efficiency the *E-field update* 2 requires 2 extra coefficients and 1 field component to be stored and requires 4 extra floating point operations to execute compared to the non-dispersive algorithm. The *RSL conductivity update*/*E-field update 1* implementation requires 2 extra coefficients and 2 field components to be stored and requires 3 extra floating point operations to execute, though its complexity is increased slightly by the "restart" procedure. Therefore where memory is important the *E-field update* 2 is preferable while the *RSL conductivity update*/*E-field update 1 implementation* is slightly quicker to execute and is preferable in situations where execution time is critical.

V. Conclusion

A number of new algorithms have been presented that enable stable simulation of dispersive media with large dielectric material values with an ADE-formulation of the FDTD equation. Two methods have been presented to model static conductivity, one as a separate dispersion term and the

other as an extension of the standard ETD-FDTD formulation. A further method has been presented that allows the stable simulation of Debye type dispersion using ETD. The accuracy of these algorithms has been demonstrated by comparison of theoretical reflection coefficient of a plane wave interacting with a material boundary with that obtain via simulation. While the generalized ATD form given in [6] is abandoned it is felt that the improvement in efficiency offered by this ADE formulation in conjunction with the ability to model a wide range of materials make these new algorithms highly attractive. Future work includes the derivation of stable formulations for other types of dispersion e.g. Lorentz and/or Drude dispersion types.

APPENDIX A: DERIVATION OF STABLE TIME DOMAIN ADE ALGORITHM FOR STATIC CONDUCTIVITY USING ETD

Define the integrating factor $e^{\int \frac{\sigma}{\varepsilon_0 \varepsilon_\infty} dt} = e^{\frac{\sigma t}{\varepsilon_0 \varepsilon_\infty}}$ and multiply (10) throughout:

$$\frac{\partial D(t)}{\partial t} \cdot e^{\frac{\sigma t}{\varepsilon_0 \varepsilon_\infty}} + \frac{\sigma}{\varepsilon_0 \varepsilon_\infty} D(t) \cdot e^{\frac{\sigma t}{\varepsilon_0 \varepsilon_\infty}} \ldots = \left(\nabla \times H(t) + \frac{\sigma}{\varepsilon_0 \varepsilon_\infty} P_{sum}(t) \right) \cdot e^{\frac{\sigma t}{\varepsilon_0 \varepsilon_\infty}} \quad (20)$$

Which simplifies due to the product rule:

$$\frac{\partial \left(D(t) \cdot e^{\frac{\sigma t}{\varepsilon_0 \varepsilon_\infty}} \right)}{\partial t} \ldots = \left(\nabla \times H(t) + \frac{\sigma}{\varepsilon_0 \varepsilon_\infty} P_{sum}(t) \right) \cdot e^{\frac{\sigma t}{\varepsilon_0 \varepsilon_\infty}} \quad (21)$$

To obtain the final solution this equation will be solved over a single iteration of the FDTD algorithm. It is assumed that over this period $\nabla \times H(t)$ and $P_{sum}(t)$ change slowly and can be approximated with constants $\nabla \times H$ and P_{sum}. This assumption is valid since the same approximation is made concerning the E field in the original FDTD algorithm and both ∇×H and P_{sum} change at the same rate. This allows both sides of (21) to be integrated with respect to *t as:*

$$\int \frac{\partial \left(D(t) \cdot e^{\frac{\sigma t}{\varepsilon_0 \varepsilon_\infty}} \right)}{\partial t} dt = \left(\nabla \times H + \frac{\sigma}{\varepsilon_0 \varepsilon_\infty} P_{sum} \right) \int e^{\frac{\sigma t}{\varepsilon_0 \varepsilon_\infty}} dt \quad (22)$$

Solving and rearranging the result to make $D(t)$ the subject:

$$D(\mathrm{t}) = \frac{\varepsilon_0 \varepsilon_\infty}{\sigma} \left(\nabla \times H(\Delta/2) + \frac{\sigma}{\varepsilon_0 \varepsilon_\infty} P_{sum}(\Delta/2) \right) + c \cdot e^{\frac{-\sigma t}{\varepsilon_0 \varepsilon_\infty}} \quad (23)$$

c may be found by finding applying the initial condition to (23) and rearranging the result:

$$D(0) = \frac{\varepsilon_0 \varepsilon_\infty}{\sigma} \left(\nabla \times H + \frac{\sigma}{\varepsilon_0 \varepsilon_\infty} P_{sum} \right) + c \cdot e^0 \quad (24)$$

$$c = D(0) - \frac{\varepsilon_0 \varepsilon_\infty}{\sigma} \left(\nabla \times H + \frac{\sigma}{\varepsilon_0 \varepsilon_\infty} P_{sum} \right) \quad (25)$$

Substituting (25) into (23) and rearranging gives the final solution:

$$D(\mathrm{t}) = D(0) \cdot e^{\frac{-\sigma t}{\varepsilon_0 \varepsilon_\infty}} + \frac{\varepsilon_0 \varepsilon_\infty}{\sigma} \left(1 - e^{\frac{-\sigma t}{\varepsilon_0 \varepsilon_\infty}} \right) \ldots \times \left(\nabla \times H + \frac{\sigma}{\varepsilon_0 \varepsilon_\infty} P_{sum} \right) \quad (26)$$

This equation is discretized by setting *t*=0 at iteration n and *t=Δ* at iteration n+1. Due to the nature of the FDTD grid The values of $\nabla \times H$ and P_{sum} are sampled at n+1/2.This results in the update equation for *D* (11):

$$D^{n+1} = D^n e^{\frac{-\sigma \Delta}{\varepsilon_0 \varepsilon_\infty}} + \frac{\varepsilon_0 \varepsilon_\infty}{\sigma} \left(1 - e^{\frac{-\sigma \Delta}{\varepsilon_0 \varepsilon_\infty}} \right) \ldots \times \left(\nabla \times H^{n+\frac{1}{2}} + \frac{\sigma}{\varepsilon_0 \varepsilon_\infty} P_{sum}^{n+\frac{1}{2}} \right)$$

APPENDIX B : DERIVATION OF STABLE DEBYE TIME UPDATE EQUATION USING ETD

Define the integrating factor $e^{\int \frac{1}{\tau} dt} = e^{\frac{t}{\tau}}$ and multiply 17 throughout:

$$\frac{\partial P_d(t)}{\partial t} \cdot e^{\frac{t}{\tau}} + \frac{1}{\tau} P_d(t) \cdot e^{\frac{t}{\tau}} = \frac{\varepsilon_0 (\varepsilon_s - \varepsilon_\infty)}{\tau} E(t) \cdot e^{\frac{t}{\tau}} \quad (27)$$

The LHS of (27) simplifies due to the product rule:

$$\frac{\partial \left(P_d(t) \cdot e^{\frac{t}{\tau}} \right)}{\partial t} = \frac{\varepsilon_0 (\varepsilon_s - \varepsilon_\infty)}{\tau} E(t) \cdot e^{\frac{t}{\tau}} \quad (28)$$

As in appendix A this equation will be solved over a single iteration of the FDTD algorithm and the assumption is made that $E(t)$ changes slowly over and can be approximated with the constant value E. This assumption is valid since the same approximation is made concerning the E field in the original FDTD algorithm. This allows both sides of (28) to be integrated with respect to *t as:*

$$\int \frac{\partial \left(P_d(t) \cdot e^{\frac{t}{\tau}} \right)}{\partial t} dt = \frac{\varepsilon_0 (\varepsilon_s - \varepsilon_\infty)}{\tau} E \int e^{\frac{t}{\tau}} dt \quad (29)$$

Rearranging to make $P_d(t)$ the subject:

$$P_d(t) = \varepsilon_0 (\varepsilon_s - \varepsilon_\infty) E + c \cdot e^{\frac{-t}{\tau}} \quad (30)$$

c may be found by finding applying the initial condition to (31) and rearranging the result:

$$P_d(0) = \varepsilon_0 (\varepsilon_s - \varepsilon_\infty) E(0) + c \cdot e^0 \quad (31)$$

$$c = P_d(0) - \varepsilon_0 (\varepsilon_s - \varepsilon_\infty) E(0) \quad (32)$$

Substituting (32) into (30) and rearranging gives the final solution:

$$P_d(t) = P_d(0) \cdot e^{\frac{-t}{\tau}} - \varepsilon_0(\varepsilon_s - \varepsilon_\infty)\left(1 - e^{\frac{-t}{\tau}}\right)E(0) \qquad (33)$$

This equation is discretized by setting t=0 at iteration n and t=Δ at iteration n+1. The value of E is sampled at iteration n. This results in the Debye update equation for P_d (18):

$$P_d^{n+1} = P_d^n \cdot e^{\frac{-\Delta}{\tau}} + \varepsilon_0(\varepsilon_s - \varepsilon_\infty)\left(1 - e^{\frac{-\Delta}{\tau}}\right)E^n$$

ACKNOWLEDGEMENT

The authors thank all at the Toshiba's Telecommunications Research Laboratory for their help and support with this work.

REFERENCES

[1] Stogryn, A., "Equations for Calculating the Dielectric Constant of Saline Water (Correspondence)," *Microwave Theory and Techniques, IEEE Transactions on* , vol.19, no.8, pp.733,736, Aug. 1971

[2] S. Gabriel, R. Lau and C. Gabriel, "The dielectric properties of biological tissues: III. Parametric models for dielectric spectrum of tissues", *Phys. Med. Biol*., vol. 41, pp. 2271–2293, 1996.

[3] Kane Yee, "Numerical solution of initial boundary value problems involving Maxwell's equations in isotropic media," *Antennas and Propagation, IEEE Transactions on* , vol.14, no.3, pp.302,307, May 1966

[4] D. M. Sullivan, "Nonlinear FDTD formulations using Z transforms," *IEEE Trans. Microw. Theory Tech.*, vol. 43, no. 3, pp. 676–682, Mar. 1995.

[5] R.J., Luebbers; F. Hunsberger, "FDTD for Nth-order dispersive media," *IEEE Transactions on Antennas and Propagation*, vol.40, no.11, pp.1297, 1301, Nov 1992.

[6] M. A. Alsunaidi and A. A. Al-Jabr, "A General ADE-FDTD Algorithm for the Simulation of Dispersive Structures," *IEEE Photonics Technology Letters*, vol. 21, no. 12, pp. 817–819, Jun. 2009.

[7] R. M. Joseph, S. C. Hagness, and A. Taflove, "Direct time integration of Maxwell's equations in linear dispersive media with absorption for scattering and propagation of femtosecond electromagnetic pulses," *Opt. Lett*. 16, pp. 1412-1414, 1991.

[8] Taflove, A.; Hagnes S.C.; "Computational Electrodynamics," Artech house, Boston, 3rd edition, 2005.

[9] Weedon, W.H.; Rappaport, C.M., "A general method for FDTD modeling of wave propagation in arbitrary frequency-dispersive media," *Antennas and Propagation, IEEE Transactions on* , vol.45, no.3, pp.401-410, Mar 1997

[10] Okoniewski, M.; Mrozowski, M.; Stuchly, M.A., "Simple treatment of multi-term dispersion in FDTD," *Microwave and Guided Wave Letters, IEEE* , vol.7, no.5, pp.121-123, May 1997.

[11] M. Okoniewski and E. Okoniewska, "Drude dispersion in ADE FDTD revisited", IET Electronics Letters," vol. 42, no. 9, pp. 9–10, 27th April 2006.

[12] S. M. Cox, P. C. Matthews, "Exponential time differencing for stiff systems", Journal of Computational Physics, 176, pp. 430-455, 2002.

[13] L. F. Shampine, "Stability of the leapfrog/midpoint method," *Applied Mathematics and Computation*, vol. 208, no. 1, pp. 293–298, Feb. 2009.

[14] G. Akrivis, M. Crouzeix, C. Makridakis, "Implicit-explicit multistep methods for quasilinear parabolic equations" *Numerical Mathematics*, vol. 82, pp 521-541, 1999.

[15] C. W. Gear and Ioannis G. Kevrekidis, "Projective Methods for Stiff Differential Equations: Problems with Gaps in Their Eigenvalue Spectrum", *SIAM J. Sci. Comput.*, 24, 4, April 2002

[16] L.F.M. Silva, H. Altenbach, "Materials with complex behavior: modelling, simulation, testing and application", Springer, 2010, pp 100-101.

[17] P. G. Petropoulos, "Analysis of exponential time-differencing for FDTD in lossy dielectrics," *IEEE Transactions on Antennas and Propagation*, vol. 45, no. 6, pp. 1054–1057, Jun. 1997.

[18] J. D. Kraus, "Electromagnetics", Fourth Edition, McGraw-Hill International Editions, New York, 1992.

David Gibbins Was Born in Brecon, Wales in 1982. In 2004 he received an M.Eng. degree in aerospace engineering from Liverpool University (U.K.). In 2009 He was awarded a PhD by the University of Bristol, on the topic of UWB antenna and microwave imaging.
From 2009-2012 he was a Research Assistant at the University of Bristol where he was a member of the Bristol's Breast Cancer Imaging Project. His involvement in this project included antenna and imaging hardware design and modelling, experimental testing as well as being part of the team running clinical trials. He is currently a member of the Toshiba Research Laboratory in Bristol where he is continuing to work in the area of medical imaging. His research interests include Biological phantoms, wide-band antenna, microwave imaging and electromagnetic simulation.
Dr Gibbins is a member of the IET.

Chris Railton received the B.Sc. degree in physics with electronics from the University of London, London, U.K., in 1974 and the Ph.D. degree in electronic engineering from the University of Bath, North East Somerset, U.K., in 1988.
During the period 1974–1984, he worked in the scientific civil service on a number or research and development projects in the areas of communications, signal processing, and EMC. Between 1984 and 1987, he worked at the University of Bath on the mathematical modelling of boxed microstrip circuits. He currently works in the Centre for Communications Research at the University of Bristol, Bristol, U.K., where he leads the Computational Electromagnetics group which is engaged in the development of new algorithms for electromagnetic analysis and their application to a wide variety of situations including planar and conformal antennas, microwave and RF heating systems, radar and microwave imaging, EMC, high-speed interconnects, and the design of photonic components.

Ian J. Craddock is full Professor at the University of Bristol, UK and Director of the flagship "SPHERE" IRC. He has been working in RF medical imaging for 10 years and he founded a company that is currently completing regulatory approval of a commercial RF breast imaging device. He has published well over 100 papers. He serves on the Steering Board of the University's Health Research Institute. He is also separately employed by Toshiba as Managing Director of their Telecommunications Research Lab in Bristol,

responsible for a portfolio of both internal and collaborative communications, healthcare and smart city research.

Tommy Henriksson (M'08) was born in Ramundeboda, Sweden, in 1978. He received the M.Sc. degree in electrical engineering and the Licentiate of Engineering degree in electronics in 2003 and 2007, respectively, from Mälardalen University, Västerås, Sweden. He received a joint French-Swedish Ph.D. degree in physics and electronics from the Universitié Paris-Sud 11, Paris, France, and Mälardalen University in 2009, with the dissertation entitled "Contribution to Quantitative Microwave Imaging Techniques for Biomedical Applications."
Investigated non-iterative algorithms for eddy-current nondestructive testing of conductive materials, with the Department of Electromagnetic Research, Laboratoire des Signaux et Systèmes,Gif-sur-Yvette, France, in 2010. Since 2011, he has been a Postdoctoral researcher with the University of Bristol, U.K. As a member of the microwave imaging team his work focuses on UWB time-domain microwave imaging techniques for solving the inverse scattering problem in medical microwave imaging. His research interests include microwave tomography and radar based imaging for biomedical and industrial applications, electromagnetic modelling, microwave imaging system realization and calibration.